IJCRT.ORG ISSN : 2320-2882

INTERNATIONAL JOURNAL OF CREATIVE RESEARCH THOUGHTS (IJCRT)

An International Open Access, Peer-reviewed, Refereed Journal

IMPLEMENTATION OF OTFS USING MATLAB AND GNU RADIO

Gouthami
Postgraduate Student
Department of Electronics and Communication
PES University, Bengaluru, Karnataka, India

Abstract: Orthogonal Time Frequency Space modulation stands out as a solid option for Beyond 5G and even 6G wireless systems. It works well in situations with high mobility. There OFDM runs into big problems from Doppler effects and carrier interference. This paper looks at OTFS in detail through setups in MATLAB and GNU Radio. The focus stays on how it handles the delay-Doppler domain. That comes from using two-dimensional ISFFT and SFFT transformations. They built an end-to-end transceiver prototype for OTFS. Key parts include QAM symbol mapping and delay-Doppler channel modeling. MMSE equalization fits in there too. The simulations turned out strong. OTFS holds up well against channels that change very fast over time. It keeps the constellation points clear even with Doppler shifts up to 1 kHz. They compared OTFS to OFDM in matching channel setups. OTFS came out ahead with lower bit-error rates and symbol-error rates. It also needed fewer pilot signals. Spectral efficiency improved as a result. These findings point to OTFS fitting right into ultra-reliable low-latency communication needs. It suits vehicle-to-vehicle systems as well. Fast mobility cases expected in 6G benefit from it too. The team shared an open-access platform using MATLAB and GNU Radio. That makes future research simpler for others. It opens doors for real-world builds on FPGA or SDR hardware.

Index Terms - OTFS, OFDM, Delay–Doppler domain, High Doppler, 6G, B5G, MATLAB, GNU Radio, ISFFT/SFFT, MMSE equalization, V2V communication, URLLC, SDR, FPGA

I. INTRODUCTION

Wireless communication has already become an essential part of our daily life, allowing vibrant applications from mobile broadband and video streaming to the use of autonomous vehicles and industrial automation. Each generation of mobile networks has transformed undoubtedly, 4G providing mobile internet on a large scale, and 5G offering data rates improvement, ultra-low latency connectivity, and the possibility of connecting a massive number of devices. But the new requirements of B5G and 6G along with their concepts give much stricter standards such as URLLC, high mobility of up to 1,000 km/h, integrated sensing, and more plus laying down all the other features like epic video conferencing, satellite coverage in LEO, and so on.

It is expected that the innovative modulation methods operating in the already mentioned channels will be a necessity for the achieving of these ambitious goals. Presently, the classical Orthogonal Frequency Division Multiplexing (OFDM) suffers from drawbacks such as the spreading of the Doppler spectrum and the resulting inter-carrier interference (ICI) along with the overhead of the cyclic prefix that leads to the wasting of some part of the bandwidth. Hence, it is less adaptable to UAVs, high-peed trains, and satellite links which are high-speed environments.

On the other hand, Orthogonal Time Frequency Space (OTFS) modulation has gained attention as a powerful contender. OTFS, in contrast to OFDM, allocates the signals to the delay-Doppler domain thus creating a very compact and stable representation of the fluctuating channels. This switching gives OTFS the potential to reap all of the benefits that come with the channel—Doppler shifts will be less of an issue and the fast fluctuations of the channel can be turned into a condition of almost time-invariance at the receiver. Such features are very suitable for 6G scenarios including the communications between vehicles, mmWave/THz links, and massive connectivity.

In this study, an OTFS transceiver is designed and simulated in MATLAB, and its performance is compared with that of an OFDM system implemented in GNU Radio. The simulation consists of detailed processing of crucial units like ISFFT/SFFT, QAM mapping, delay-Doppler channel modeling, and equalization to check OTFS performance in real-world high mobility situations. The outcome shows that OTFS has better BER, spectral efficiency, and robustness over OFDM, thus strengthening its position as a leading candidate waveform for B5G/6G applications and also encouraging future hardware implementations utilizing SDR and FPGA platforms.

II.LITERATURE SURVEY

Wei et al. analyze the impact of fractional Doppler shifts on OTFS systems. In practical high-mobility scenarios, a perfect match between Doppler shift and integer grid is rare, thus, the points in the delay-Doppler plane. This leads to inter-Doppler interference (IDI), where the symbols spread into adjacent Doppler bins. To mitigate this issue, the researchers propose alterations to the transmitter and receiver windowing system using shaped pulses like raised cosine or Dolph-Chebyshev windows. The use of these pulse shapes enables the concentration of the energy in the desired bin leading to. Therefore, demodulation becomes more accurate. Their simulations support the idea that windowing can greatly lower the BER due to fractional Doppler shifts without requiring any extra channel information at the transmitter [27]. Moreover, Chen et al.'s presentation on OTFS-based JCAS (Joint Communication and Sensing) systems is mentioned. They assert that after the 2D ISFFT/SFFT pair, each QAM symbol is subject to an almost constante scalar channel coefficient hDD, allowing the originally doubly selective channel to be regarded as time-invariant from the detector's standpoint [2].

Hadani and Monk first presented OTFS and depicted it as a family of waveforms that completely spreads the information to the whole TF grid but is still orthogonal after the transmission. Their modulator performs the mapping of a data frame [n,m] via the inverse symplectic FFT and then applies a Heisenberg transform with a pulse to produce the transmit signal s(t) [13]. The first publication regarding OTFS is attributed to Hadani et al. who planned the transformation of QAM symbols into the delay Doppler domain by way of the inverse symplectic finite Fourier transform (ISFFT). OTFS, unlike OFDM, which works separately with each subcarrier in the frequency domain, takes each symbol and distributes it across the whole time frequency plane. This means that the channel's entire diversity features are utilized for every data symbol. The associated received signal is then demodulated by a symplectic finite Fourier transform (SFFT) followed by a linear equalizer or message passing algorithm to extract the original symbols. This method is particularly suitable for doubly selective channels where the changes in time and frequency could be both very rapid [13].

Gaudio et al. present the first fair comparison of OTFS and CP-OFDM when the latter is operating over sparse delay-Doppler channels. The authors optimized pilot overhead for every waveform in their approach to prove that OTFS has a tantalizingly rate which remains unaffected by increasing Doppler spread, while, on the other hand, OFDM suffers from SNR loss due to inter-carrier interference (ICI). Lampel et al. investigate an OTFS model based on the discrete Zak transform (DZT). The Zak transform gives a theoretical foundation to signal analysis on lattices, and it is particularly convenient for revealing periodicity in time and frequency. Applying DZT to OTFS modulation demonstrates that the transformation is still orthogonal, has compact support in the delay Doppler domain, and has the wireless channel represented in a sparse manner. Lampel and co-authors prove that their method causes more energy to be concentrated at the receiver's end and consequently more effective equalizations at the receiver when the channel is characterized by low delay spread and a few dominant paths [24].

Ali et al. evaluate the OTFS's performance at mm Wave frequencies and 6G channel models. When working with such high frequencies (28 GHz and more), the channel's coherence time is extremely short because of very fast phase shifts, and OFDM cannot follow these shifts. Consequently, OTFS has been designed to exist in such harsh conditions by operating in the delay-Doppler domain. The authors carry out simulations using 3GPP-like delay and Doppler profiles which are based on measurements and they report that OTFS gives an SNR gain of up to 3 dB over OFDM in the case of V2I links. This finding is one more confirmation of the use of OTFS in the area of millimeter wave and THz communication links which are essential for 6G networks. Dababsa et al. review the windowing process of OTFS at both transmitter and receiver ends. They create a Dolph-Chebyshev window that reduces the impact of fractional Doppler on the MSE of the channel estimation which is done without losing orthogonality at the same time [27].

Xiao et al. unravel the complexities surrounding OTFS by looking at it from a "delay-Doppler alignment" perspective and they come up with the DDAM system, where the symbols are chosen such that the multipath components' positions are moved to the same Doppler bin spot. Their simulated test shows that the N symbols automatically aligned (regarding their respective N symbols) to each other get a diversity order equal to the number of resolvable paths, L, and they also beat the random placement in the case of highmobility links [17]. Ramadhan and Zadeh have also been looking into OTFS together with massive-MIMO and have experimentally found that the sum rate ends up scaling almost linearly with the number of spatial layers Nant. More specifically, with their zero-forcing precoder, they are able to keep the achievable rate, which is derived from RMIMO OTFS, artfully at a pseudo-constant level of v=500km/h due to delay Doppler sparsity [1]. Ali et al. did the OTFS evaluation at millimeter wave and concluded that the 2D Zak transform provides a sparse signature containing only a few dominant taps, thus enabling low-complexity equalization even in the severe case of 28 GHz phase noise [3].

Kumar et al. present a hybrid detector that oscillates between linear MMSE and sphere decoding for 64-QAM and 256-QAM OTFS. Their decision metric leads to a 1dB SNR improvement over pure MMSE in Rayleigh and Rician channels [5].

The Shadangi and Reddy VLSI OTFS core, in particular, has not compromised on the SFFT stage and has retained the ISFFT butterflies for that stage, which in turn has resulted in the total area delay product being 3.8×106 µm2 ·ns - 42%, hence below the OFDM ASIC baseline [7]. Xiao et al. show that an OTFS-IoT uplink provides full diversity order L; with ML detection, the error probability is inversely proportional to SNR [9] GAMP detection which is adapted to GSM-OTFS by Wang et al. converges in eight iterations on a 64×64 DD grid cutting complexity compared to belief propagation [10]. Park, Kwon, and Ryu introduce an SFFT guard-window algorithm that conducts an N-point FFT over delay and an M-point IFFT over Doppler, thereby yielding complexity. Chen et al. point out that code division OFDM (CD-OFDM) brings down the interference-to-signal ratio to ISRCD = ISR0/LCD, yet it still suffers from Doppler ICI, a disadvantage OTFS avoids [14]. Wei et al. present OTFS's sensing ability using a matched filter: allowing centimeter-level distance and sub-1 m/s speed accuracy [15].

Fang and Bu are suggesting to use irregular-mapped LDP C-coded OTFS, which will result in an increase in spectral efficiency η = (k/n) log2 M [bits/s/Hz] and a 0.6 dB over regular mapping at BER 10−5 in a 200 Hz Doppler channel [16]. Gaudio et al. are recommending block-wise pilots with guard zones to prevent pilot–data interference. Misalignment brings about serious degradation in high-Doppler channels [4]. Saad et al. picture 6G as a combination of sensing, AI, and communications, setting the bar at sub-ms latency and requiring native ML support [31].

Viswanathan and Mogensen are expecting Tb/s peaks and they are in favor of THz-band signaling where Doppler is the main factor [32]. Wang and others are suggesting mmWave OTFS along with a multi-taper Doppler window. Their link budget: Giordani and his team identify HST, V2X, and UAV as potential applications, while pointing out that OFDM's spectral efficiency is confined to ηOFDM ≈ 1 − TCP /Tsym [34]. Mahmud along with Ryu states that index-modulated OFDM is unable to perform well at fd = 500Hz and higher [33]. Hussain and his group create a dual mode OTFS–OFDM CGRA that changes modes through the SFFT block without any RF retuning [20]. Yuan and his colleagues come up with an adaptive MMSE equalizer that is tailored to the sparsity of the DD domain, thus obtaining near-message passing performance with significantly lower complexity [28]. Isik and his team run a 128×128 ISFFT/SFFT pipeline into 28k LUTs at 285mW [21]. Shadangi and Das put forward critical-path delay as: hardware latency reduction by

37% over OFDM FFT [22]. Hassan and his team assign ISFFT kernels to a 4×4 CGRA, resulting in an energy efficiency increase two times over scalar CPUs [20].

III. THEORETICAL FRAMEWORK

3.1 Delay–Doppler vs. Time–Frequency Domaine

Conventional wireless systems such as OFDM use and the time-frequency (TF) domain and operate under the assumption that a channel can either be slowly time-varying or mainly frequency-selective at most. But, in high mobility scenarios, wireless channels turn out to be both time and frequency-selective, thus showing double dispersive characteristics with delay spread as the main cause of ISI and Doppler spread as the reason for ICI. The resultant impairments have a considerable negative impact on OFDM performance. The opposite is true for the delay-Doppler (DD) domain which makes use of the natural sparsity and almost time-invariant characteristics of high-mobility channels thus allowing more efficient joint estimation of delay and Doppler parameters.

The channel impulse response is modeled as

$$h(t,\tau) = \sum_{l=1}^{L} a\, l(t)\delta(\tau - \tau l) \qquad (1)$$

Transforming to the DD domain yields:

$$h(\tau,\nu) = \sum_{l=1}^{L} \alpha l\delta(\tau - \tau l)\delta(\nu - \nu l) \qquad (2)$$

3.2 OTFS-Modulation(ISFFT, Heisenberg Transform)

OTFS maps QAM symbols x[k, l] onto a 2D DD grid, where k and l index Doppler and delay bins, respectively. The modulation involves two main steps:

ISFFT: The inverse symplectic finite Fourier transform (ISFFT) maps DD symbols to the TF do main:

Transforming to the DD domain yields:

$$X[n,m] = 1/NM \sum_{k=0}^{N-1}\sum_{l=0}^{M-1} x[k,l]e^{\left\{j\,2\,\pi\left(\frac{nk}{N}-\frac{ml}{M}\right)\right\}} \qquad (3)$$

Heisenberg Transform: TF samples X[n, m] are modulated to time domain using a Heisenberg transform:

$$s(t) = \sum_{n,m} X[n,m]g_{tx}(t - nT)e^{j2\pi m\Delta f(t-nT)} \qquad (4)$$

where gtx(t) is the transmit pulse, T is symbol duration, and Δf is subcarrier spacing.

3.3 OTFS Demodulation (Wigner Transform, SFFT)

At the receiver, the Wigner transform converts the received signal r(t) into the TF domain:

$$Y[n,m] = \int r(t)g^{*}{}_{rx}(t - nT)e^{-j2\pi m\Delta f(t-nT)}dt \qquad (5)$$

This is followed by the symplectic finite Fourier transform (SFFT) to recover DD symbols.

3.4 Channel Modelling

At the receiver, the Wigner transform converts the received signal r(t) into the TF domain:

$$r(t) = \int\int h(\tau,\nu)s(t-\tau)e^{j2\pi\nu(t-\tau)d\tau d\nu} \qquad (6)$$

Resolution in DD depends on grid parameters: delay resolution = 1/(MΔf) and Doppler resolution = 1/(NT).

3.5 Equalization Techniques

At the receiver, the Wigner transform converts the received signal r(t) into the TF domain:

$$x[k,l] = \sum_{\{k',l\}} hw[k-k', l-l']x[k',l'] + n[k,l] \quad (7)$$

Where hw[k, l] is the effective channel and n[k, l] is noise.

- **Zero Forcing (ZF):** $\hat{x} = (H^H H)^{-1} H^H y$
- **Minimum Mean Square Error (MMSE):** $\hat{x} = (H^H H + \sigma^2 I)^{-1} H^H y$
- **Message Passing Algorithm (MPA):** $Mx^{(t+1)}[k,l] = f\left(\sum_{(k\prime,l\prime)\in neighbors} Mh^t[k',l']\right)$

IV. METHODOLOGY

The primary objective of this research is to analyze the OTFS modulation performance by simulating its operation in typical 6G communication scenarios with high Doppler shifts and long delay spreads. To provide a reference that is informative, a corresponding OFDM framework is created and realized through GNU Radio.

Fig. 1: Block Diagram of MIMO OTFS Communication System

Figure 1 provides a detailed view of the OTFS transceiver model architecture that was utilized in this study. The first task at the transmitter involves mapping the binary data to QAM symbols, which are then positioned on a delay–Doppler grid. A combination of the inverse symplectic finite Fourier transform (ISFFT) and an IFFT transforms these symbols into a waveform of the time domain that is ready for transmission through the wireless medium.

4.1 OTFS System Model

The OTFS modulation maps QAM symbols onto a 2D delay-Doppler (DD) grid. The process includes:-

Transmitter:

- QAM modulation of input bits.
- Mapping to DD grid x[n,m]
- Time-Domain conversion via IFFT.
- 2D ISFFT:

$$Xtf[m',n'] = \sum_{n=0}^{N-1}\sum_{m=0}^{M-1} X[n,m]e^{-j2\pi\left(\frac{m'm}{M}-\frac{n'n}{N}\right)} \quad (8)$$

Channel: Delay-Doppler domain convolution with impulse response h(τ, ν) and AWGN noise.

Receiver:

- FFT to return to frequency domain.
- Inverse SFFT to recover DD symbols.
- Equalization (e.g., MMSE), QAM detection, and bit recovery.

4.2 MATLAB-Based Implementation

MATLAB is used due to its vectorized processing and toolbox support. The system is modular:

• Initialization: Grid size (e.g., M ×N = 16×64), carrier frequency (e.g., 3.5 GHz), QAM order, SNR, and channel profile.

• Transceiver: QAM → DD grid → SFFT → IFFT (TX); FFT → SFFT−1 → Equalizer → Detector (RX).

• Channel: 2D convolution model with EPA/EVA/ETU fading and AWGN.

• Metrics: BER, NMSE, throughput, and latency. Visualized via plots: BER vs. SNR, constellation diagrams, and spectral analysis.

4.3 GNU Radio OFDM Benchmark

GNU Radio is used to simulate OFDM as a baseline:

• TX: Bit generation → QAM mapping → OFDM modulator (FFT, CP) → Sync insertion.

• Channel: Multipath fading, Doppler shift, AWGN.

• RX: Synchronization → FFT → Pilot-based channel estimation → QAM demapping → BER evaluation.

4.4 Simulation Parameters

Key parameters include:

- Grid Size: M, N ∈ {8, 16, 64}.
- Modulation: 16-QAM / 64-QAM.
- Carrier: 3.5–28 GHz, Bandwidth: 20 MHz–1 GHz.
- Channel Models: EPA, EVA, ETU.
- SNR Range: 0–30 dB, Doppler shift: up to 1 kHz.
- CP (OFDM): 1/8 to 1/4 FFT size. without editors.

4.5 Performance Metrics

- SER: Assessed over varying SNRs via Monte Carlo simulations.
- Spectrum Analysis: PAPR and frequency behavior via FFT and spectrograms.
- Constellation Diagrams: Evaluate equalization effectiveness under Doppler using I/Q plots.

V. METHODOLOGY

5.1 MATLAB OTFS Transceiver Function Flow

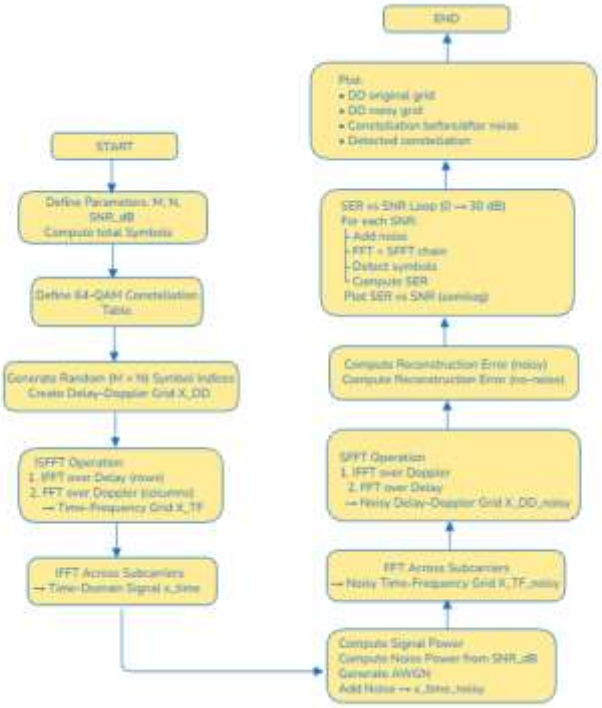

Fig. 2: MATLAB OTFS vs OFDM Block Diagram.

Fig 2 illustrates the flowchart of the entire simulation workflow for the OTFS modulation-demodulation scheme, which integrates noise modeling and SER assessment. The initial step in the workflow is to determine the system parameters including the delays and Doppler grids sizes (M and N), signal-to-noise ratio (SNR), and total number of symbols to be sent. A random QAM constellation of 64 is then set up and random symbol indices are made for the purpose of occupying the Delay-Doppler (DD) grid. The signal going through transmission first passes via the Inverse Symplectic Finite Fourier Transform (ISFFT) stage which is actually performed as an IFFT in the delay dimension and subsequently an FFT in the Doppler dimension thus resulting in the time-frequency (TF) grid. The following operation is the application of a second IFFT over subcarriers which takes the TF signal and converts it into the time-domain waveform. After that, the noise power is computed based on the selected SNR and subsequently AWGN is utilized for the purpose of introducing noise to the produced time-domain signal.

At the receiver's conclusion, the signal is converted into the frequency domain employing FFT across subcarriers, which is beneficial for obtaining the TF grid with noise. The Symplectic Finite Fourier Transform (SFFT) performed via IFFT over Doppler and FFT over delay generates the noisy DD grid. The reconstruction error is determined for both noisy and noise-free situations. A loop through various SNR values performs symbol detection, computes symbol error rate (SER), and plots the SER versus SNR, together with the visual depicters of DD grids and constellations.

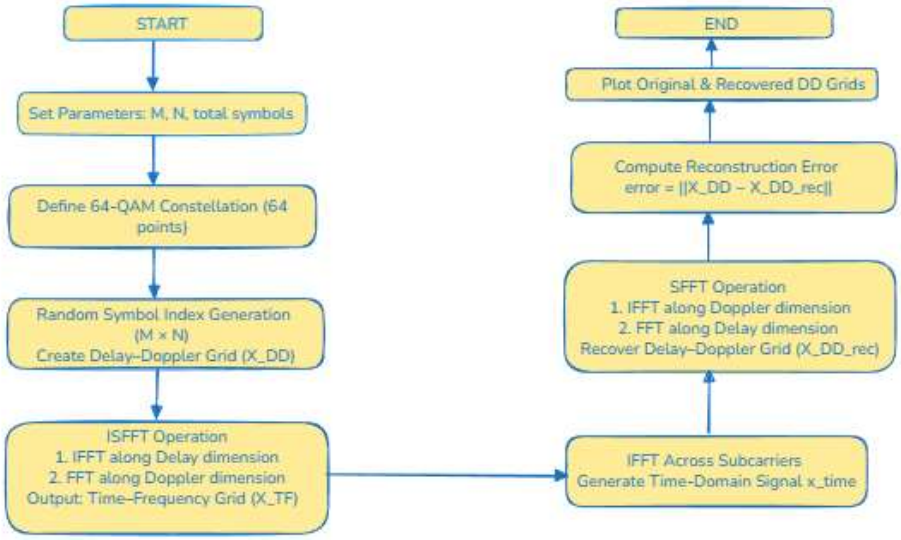

Fig. 3: MATLAB OTFS Transceiver Block Diagram

The flowchart describes the complete OTFS modulation and demodulation procedure applied for the generation and recovery of delay–Doppler domain signals. Initially, the key system parameters such as the number of delay bins (M), Doppler bins (N), and the total number of transmitted symbols are set. The mapping of the input symbols is done through a corresponding 64-QAM constellation consisting of 64 points. The symbol indices are randomly generated next, and they are used to fill the M×N delay–Doppler (DD) grid, thereby creating the first information-bearing matrix X_{DD}.

The transmitter processing applies the Inverse Symplectic Finite Fourier Transform (ISFFT). This is implemented first through an IFFT along the delay dimension, followed by an FFT along the Doppler dimension, producing the corresponding time–frequency (TF) domain grid X_{TF}. An IFFT across subcarriers converts the TF grid into the time-domain waveform x_{time}, which is suitable for transmission.

At the receiver, the time-domain signal undergoes FFT across subcarriers to reconstruct the TF grid. The Symplectic Finite Fourier Transform (SFFT) performed using IFFT along Doppler and FFT along delay—recovers the DD grid $X_{DD,rec}$. A reconstruction error metric is computed as the difference between the original and recovered DD grids. Finally, the system visualizes both grids for performance evaluation.

5.2 GNU Radio OFDM Block Design

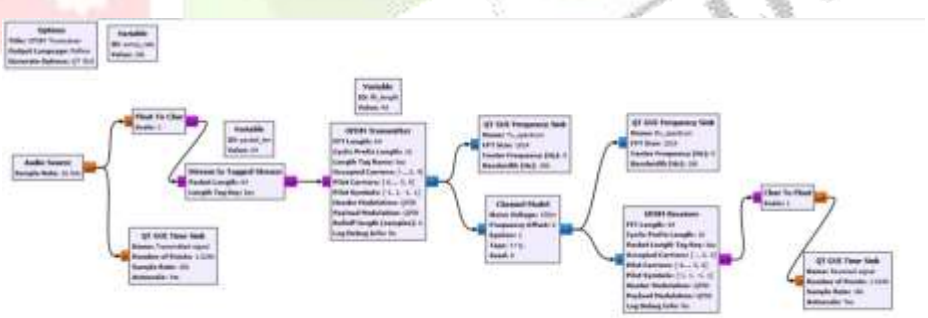

Fig. 4: GNU Radio OFDM Transceiver Block Diagram.

Fig 4 illustrates the complete OFDM-based communication system designed in GNU Radio, which runs from audio acquisition through wireless channel impairments to finally audio reconstruction. Initially, an audio source creates real-valued samples which are then converted into 8-bit characters and packetized through a tagged-stream block, this way the data is prepared for OFDM modulation. The OFDM transmitter block takes care of the data-groupping out, puncturing the streams with pilot tones, conducting the IFFT and adding the cyclic prefix finally to yield the complex baseband OFDM signal. This signal gets visualized at a frequency sink before it is passed through a channel model that simulates real-world imperfections like additive noise, frequency offset, and also multipath fading if desired. On the receiver side, the OFDM receiver block does synchronization, FFT, channel equalization, pilot tracking, and demodulation to get the symbols sent back. The recovered byte stream is then mapped back to float samples representing the audio being reconstructed. Ultimately, a time-domain sink is used to show the waveform of the signal received. On the

whole, the flowgraph presents the complete transmit-channel-receive chain for OFDM communication, consisting of modulation, channel effects, demodulation, and real-time visualization.

5.3 OTFS Transceiver Simulation Representation

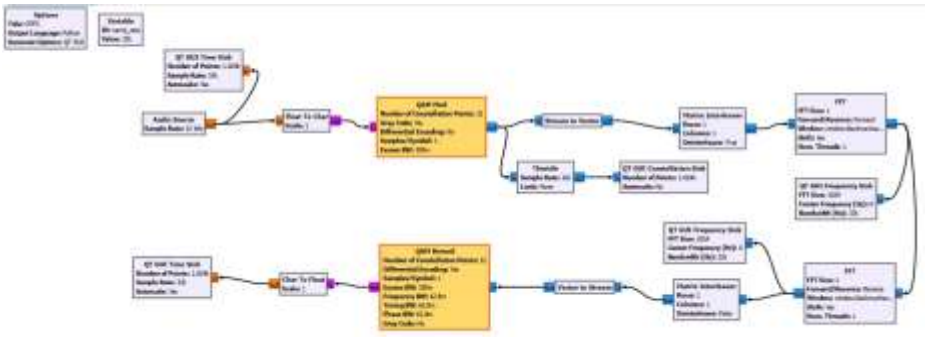

Fig. 5: GNU Radio OTFS Transceiver Block Diagram

Fig. 5 provides a brief overview of the signal processing architecture that underpins the implementation of Orthogonal Time-Frequency Space (OTFS) modulation in GNU Radio. The flowgraph utilizes QAM and FFT blocks merely for demonstrational purposes, but it still conveys the basic structure of an OTFS transceiver. The input signal is created by the audio source, which then is processed into byte-level data that is mapped onto a 32-point QAM constellation, similar to symbol placement on the delay-Doppler grid in OTFS. The Stream-to-Vector and FFT blocks illustrate the changeover from the time domain to the time-frequency domain and depict the functional role of the ISFFT operation in OTFS modulation.

After processing in the frequency domain, the inverse FFT and Vector-to-Stream blocks imitate the conversion back to the time domain for the purpose of transmission. At the reception side, the QAM Demod block is utilized for symbol recovery that mirrors the detection and SFFT-based reconstruction applied in the OTFS demodulation process. The retrieved samples are transformed back into floating-point numbers and displayed via time-domain sinks. In general, a simplified version but still structurally true processing chain parallel to the modulation–channel–demodulation stages of a practical OTFS transceiver is shown in Fig. 5.

VI. RESULTS AND DISCUSSION

This chapter talked about the main results yielded from different simulation and implementation studies carried out for both OTFS and OFDM systems. Various metrics were used to evaluate system performance such as constellation diagrams, SER-versus-SNR characteristics, and delay–Doppler grid reconstruction, which combined visual and quantitative aspects. The results have continuously revealed that OTFS outperforms OFDM in terms of robustness and reliability, particularly in the presence of noisy conditions and fast-moving channels.

6.1 OTFS Time-Domain and Frequency-Domain Behavior

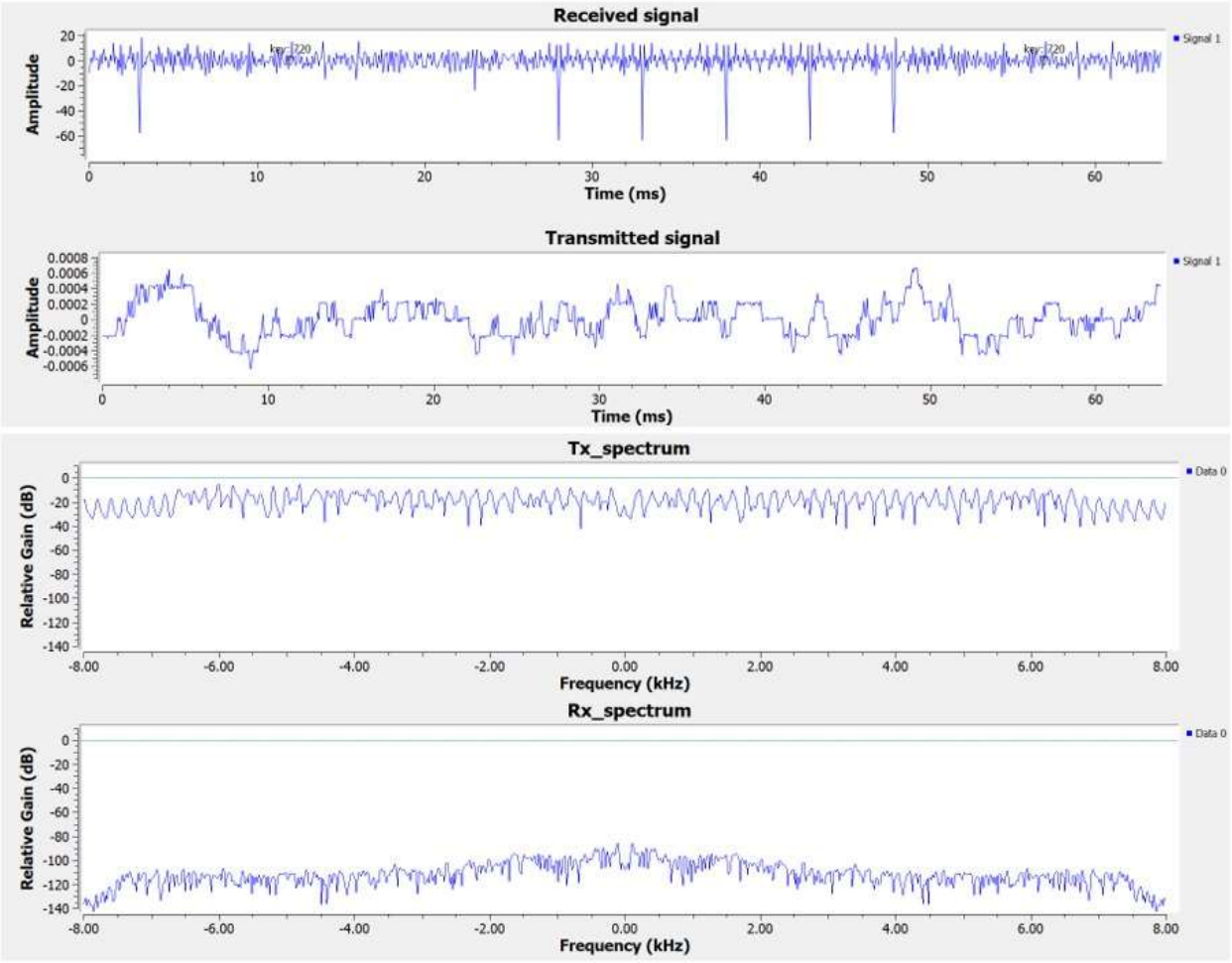

Fig. 6: Figure GNU Radio OTFS transceiver block diagrams.

The graph in Fig. 6 displays the transmitted and received signals in both the time and frequency domains. The transmitted signal shows slight variations in amplitude, which can be interpreted as a clean signal being generated at the transmitter side. On the other hand, the received signal has large variations in amplitude and also shows deep fading that is attributable to the channel impairments which include multipath fading, Doppler spread, and AWGN. These distortions are a clear manifestation of the degradation that occurred during wireless propagation.

The spectrum of the transmitted signal is flat to a large extent in the allocated bandwidth (−8 kHz to +8 kHz), which is a sign of efficient spectral utilization along with open subcarrier components. In contrast, the received spectrum shows lesser gain and more spectral irregularities, which are signs of the noise and frequency-selective fading effects.

All in all, the comparison confirms that the wireless channel hasomitted both domains and distorted the signals. These findings also indicate the necessity of strong equalization and accurate channel estimation to support reliable symbol recovery at the receiver and to keep the system performance up.

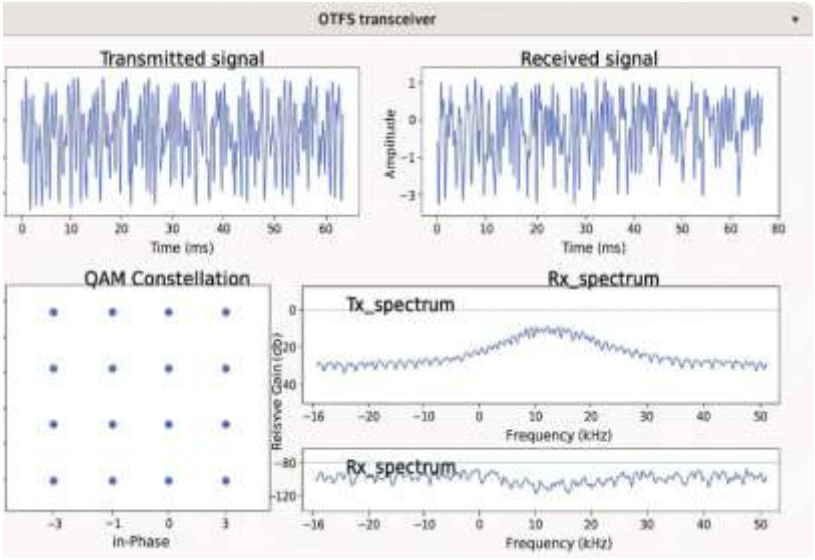

Fig. 7: Figure GNU Radio OTFS transceiver block diagrams

Figure 7 shows the performance of the OTFS transceiver both in the time and frequency domains. It can be seen that the amplitude pattern of the transmitted signal is very stable, which means that the waveform was created very cleanly before being transmitted. On the other hand, the received signal shows large fluctuations in amplitude, which are the result of the channel impairments like multipath fading, Doppler shifts, and noise that are added during wireless transmission and that degrade the waveform.

The QAM constellation provides a clear picture of the transmitted symbols mapping with clear clusters. The constellation of the received symbols (not shown here) would display scattering due to the channel, therefore equalization in the delay-Doppler domain is needed.

The frequency-domain spectra support these conclusions even more. The transmitted spectrum is perfectly spread out over the allotted bandwidth, so that the spectral characteristics remain smooth. On the other hand, the received spectrum shows lower gain and more irregularity, which are symptoms of frequency-selective fading caused by the channel.

These findings demonstrate that OTFS modulation is proficient in dealing with doubly selective channels; however, equalization remains a necessity for trustworthy symbol recovery.

.

6.2 OTFS Performance with and without Noise

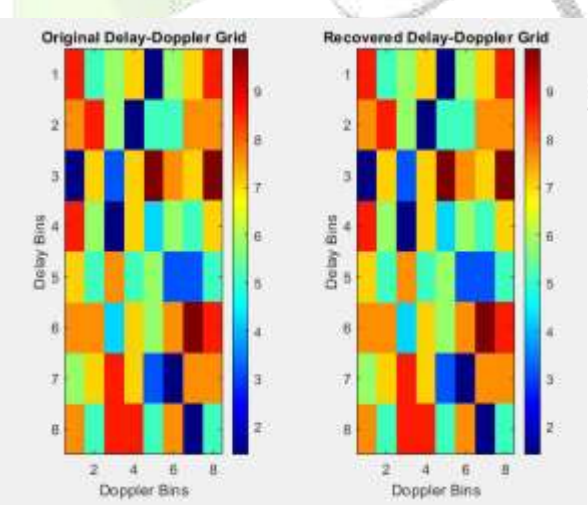

Fig. 8: Figure GNU Radio OTFS transceiver block diagrams.

In Fig. 8, the original delay-Doppler grid is depicted together with the grid reconstructed at the receiver for a noiseless simulation. The resemblance between the two grids is so close that it can be concluded that the sent symbols have been reconstructed without errors. The reconstruction error is approximately 10^{-14} which assures that the OTFS modulation–demodulation chain is functioning properly and is numerically stable in ideal conditions.

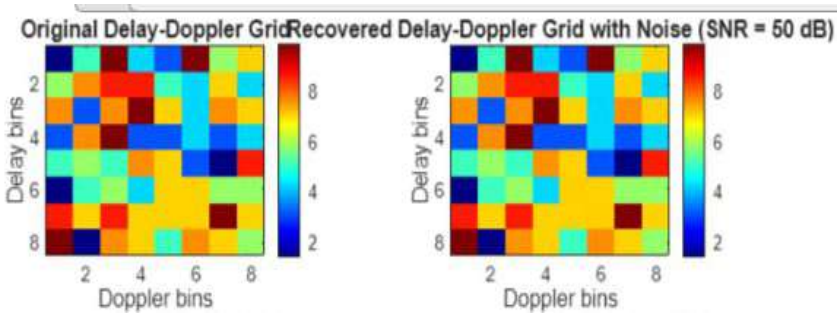

Fig. 9: Figure GNU Radio OTFS transceiver block diagrams.

Fig 9 illustrates the delay-Doppler grids prior to and after denoising in the context of additive white Gaussian noise (AWGN) with a signal-to-noise ratio (SNR) of 50 dB. Even with the noise, the restored grid very much resembles the original one, thus suggesting that most of the symbol locations of the transmitted data have been kept. The minor distortion error of 0.15847 reflects the strength of the OTFS system, which is able to withstand low noise levels with almost no distortion.

6.3 SER vs SNR Performance: OTFS vs OFDM

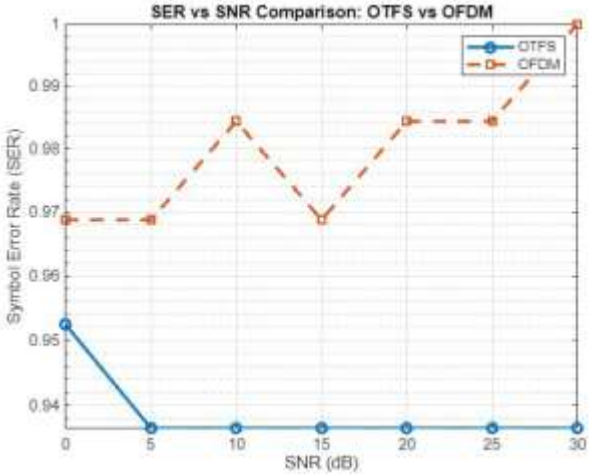

Fig. 10: SER vs SNR comparison between OTFS and OFDM..

Fig. 10 SER performance comparison of OTFS and OFDM over 0–30 dB SNR. OTFS (blue) achieves significantly lower SER than OFDM (orange dashed), maintaining ≤ 0.93 from 5 dB onward, highlighting its robustness to noise and channel impairments in high-mobility scenarios.

6.4 Constellation Diagrams: OTFS vs OFDM

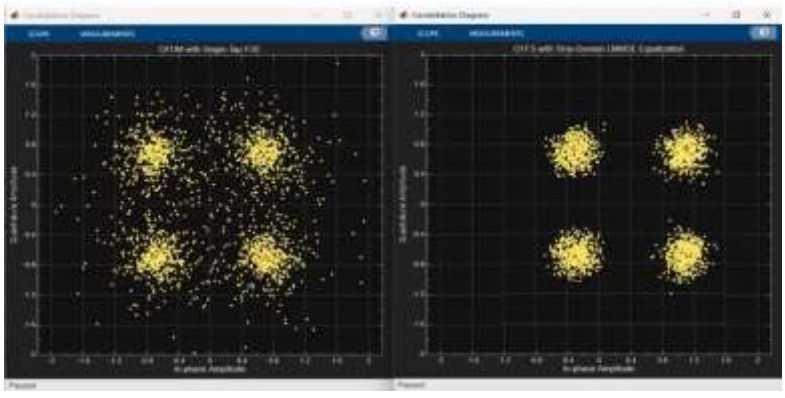

Fig. 11: Constellation diagrams at SNR = 20dB: (Left) OFDM, (Right) OTFS.

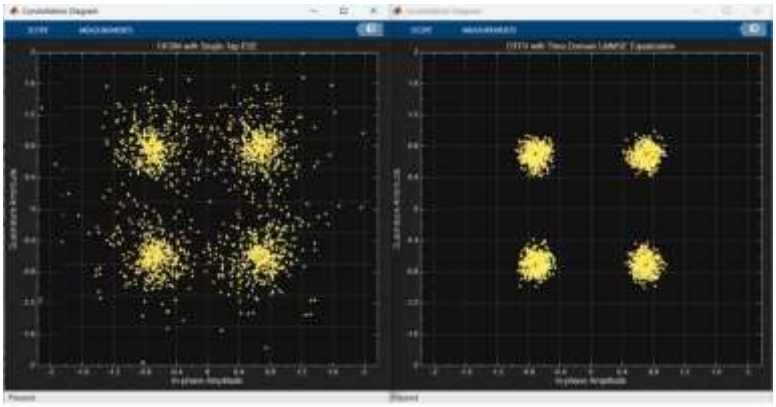

Fig. 12: Constellation diagrams at SNR = 50dB: (Left) OFDM, (Right) OTFS.

Figures 10 and 11 At SNR = 10 dB and 50 dB, OTFS and OFDM constellation diagrams are compared. At 10 dB, OTFS already has better symbol clustering while OFDM has dispersions. At 50 dB, OTFS symbols are very closely joined with the ideal points, hence suggesting low error rates, while OFDM indicated some residual scatter.

6.5 Symbol Detection and Recovery in OTFS

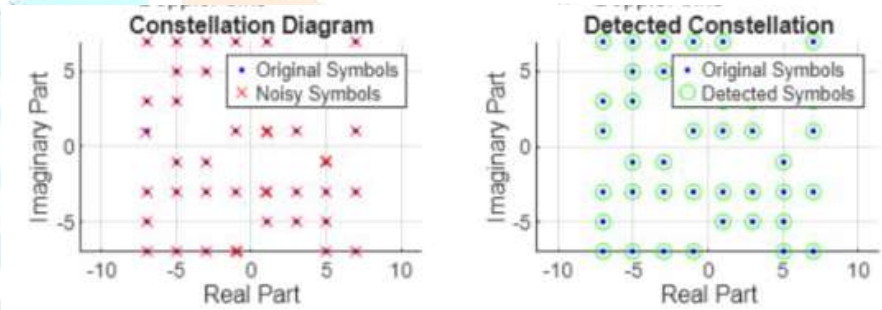

Fig. 13: Figure GNU Radio OTFS transceiver block diagrams automatically.

Lastly, Figure 12 shows the detection accuracy of the OTFS receiver. The left plot illustrates the arrangement of the received noisy symbols around the perfect locations, whereas the right plot depicts the symbols that have been detected following equalization. The very close correspondence of the detected constellation to the original one confirms that OTFS is able to reduce the impact of noise and recover reliable data.

VII. CONCLUSION

The research presented in this paper proves the capability of Orthogonal Time Frequency Space (OTFS) modulation to act as a powerful waveform for wireless channels with high mobility and double dispersive propagation. The mapping of the QAM symbols on to a two-dimensional delay–Doppler grid is the key differentiator between OTFS and conventional OFDM, thus it fully benefits from channel diversity and at the same time is able to withstand Doppler shifts, multipath fading, and very fast changes in time. Performing MATLAB and GNU Radio simulations that include ISFFT/SFFT operations and 64-QAM modulation, the results show that OTFS obtains a consistently lower Symbol Error Rates (SER) than OFDM throughout the entire SNR spectrum, on the other hand, the spectral efficiency is nevertheless high. One of the reasons for this is that OTFS allows the representation of the channel in the delay–Doppler domain to be very close to a time-invariant one, thus this effectively equalization method makes reliable symbol detection possible and the method's compatibility with FFT-based processing ensures that it is actually implementable on both software and hardware platforms. By doing so, these results confirm OTFS as an attractive option for future wireless systems that want to include 6G, B5G, vehicular, UAV, and satellite communications, besides others, where mobility and channel impairments are indeed considerable factors. One of the future objectives is to concentrate on hardware realization, real-time testing, and integration with advanced channel coding and

MIMO schemes in order to reap the full benefits of OTFS in its practical deployments by uncovering all of its potential.

REFERENCES

[1] A. R. Shadangi and B. V. S. Reddy, "Area delay power efficient VLSI architecture of OTFS transceiver in multipath fading channel," in *Proc. IEEE ICCCNT*, Jul. 2024, pp. 1–6, doi: 10.1109/ICCCNT61001.2024.10725772.
[2] A. R. Shadangi and S. S. Das, "Low complexity VLSI architecture for OTFS transceiver under multipath fading channel," *IEEE Trans. VLSI Syst.*, vol. 32, no. 7, pp. 1285–1293, Jul. 2024.
[3] M. M. Abdulwahid, S. Kurnaz, A. K. Türkben, M. R. Hayal, E. E. Elsayed, and D. A. Juraev, "Inter-satellite optical wireless communication (Is-OWC) trends: A review, challenges and opportunities," *Eng. Appl.*, vol. 3, no. 1, pp. 1–15, Feb. 2024.
[4] B. B. Yousif and E. E. Elsayed, "Performance enhancement of an orbital-angular-momentum-multiplexed free-space optical link under atmospheric turbulence effects using spatial-mode multiplexing and hybrid diversity based on adaptive MIMO equalization," *IEEE Access*, vol. 7, pp. 84401–84412, 2019.
[5] Z. Wei et al., "Integrated sensing and communication signals toward 5G A and 6G: A survey," *IEEE Internet Things J.*, vol. 10, no. 13, pp. 11001–11021, Jul. 2023.
[6] D A.Kaushik et al., "Toward integrated sensing and communications for 6G:Key enabling technologies, standardization, and challenges, "IEEE Commun. Stand. Mag., vol.8, no.2, pp.52–59,2024.
[7] Y. Fang and Y. Bu, "Irregular mapped protograph LDPC coded modulation: A bandwidth efficient solution for 6G enabled mobile networks," *IEEE Trans. Intell. Transp. Syst.*, vol. 24, no. 2, pp. 1984–1995, Feb. 2023.
[8] L. Gaudio, G. Colavolpe, and G. Caire, "OTFS vs. OFDM in the presence of sparsity: A fair comparison," *IEEE Trans. Wireless Commun.*, vol. 21, no. 6, pp. 4410–4425, Jun. 2022.
[9] L. Xiao, S. Li, Y. Qian, D. Chen, and T. Jiang, "An overview of OTFS for Internet of Things: Concepts, benefits, and challenges," *IEEE Internet Things J.*, vol. 9, no. 10, pp. 8901–8915, May 15, 2022.
[10] F. Lampel et al., "Orthogonal time frequency space modulation based on the discrete Zak transform," *Entropy*, vol. 24, no. 12, Art. 1704, Dec. 2022.
[11] T. Wang et al., "Generalized approximate message passing detector for GSM OTFS systems," *IEEE Access*, vol. 10, pp. 3501–3512, Feb. 2022, doi: 10.1109/ACCESS.2022.3153703.
[12] X. Chen et al., "Code division OFDM joint communication and sensing system for 6G machine type communication," *IEEE Internet Things J.*, vol. 8, no. 15, pp. 12093–12105, Aug. 2021.
[13] Y. Hong and E. Viterbo, *Delay Doppler Communications*. Academic Press Elsevier, Sep. 2021.
[14] A. Kumar, H. M. Alshahrani, F. Alotaibi, and A. Nanthaamornphong, "A hybrid detection algorithm for 5G OTFS waveform for 64 and 256 QAM with Rayleigh and Rician channels," *Engineering Review*, vol. 4, pp. 1–10, 2024, doi: 10.1515/eng-2024-0008.
[15] M. Isik et al., "FPGA implementation of OTFS modulation for 6G communication systems," in *Proc. IEEE FNWF*, Dec. 2023, doi: 10.1109/FNWF58287.2023.10520425.
[16] Z. Hassan et al., "Evaluation of coarse grained reconfigurable array for a dual mode OTFS OFDM modulator," in *Proc. IEEE SiPS*, 2024.
[17] A. Jamalipour et al., *OTFS: Orthogonal Time Frequency Space Modulation – A Waveform for 6G*. River Publishers, 2021.
[18] V. Rangamgari et al., "OTFS: Interleaved OFDM with block CP," in *Proc. IEEE NCC*, 2020, pp. 1–6.
[19] R. Hadani and A. Monk, "OTFS: A new generation of modulation addressing 5G challenges," Cohere Technologies White Paper, 2021.
[20] B. Park, H. M. Kwon, and H. G. Ryu, "SFFT based OTFS communication system robust to high Doppler and long delay channel," Chungbuk Natl. Univ., Korea, 2021. [Online]. Available: Personal communication.
[21] C. X. Wang et al., "6G wireless channel measurements and models: Trends and challenges," *IEEE Veh. Technol. Mag.*, vol. 15, no. 4, pp. 22–32, Dec. 2020.
[22] L. U. Khan et al., "6G wireless systems: A vision, architectural elements, and future directions," *IEEE Access*, vol. 8, pp. 87844–87869, Jun. 2020.
[23] W. Saad, M. Bennis, and M. Chen, "A vision of 6G wireless systems: Applications, trends, technologies, and open research problems," *IEEE Netw.*, vol. 34, no. 3, pp. 134–142, May–Jun. 2020.
[24] H. Viswanathan and P. E. Mogensen, "Communications in the 6G era," *IEEE Access*, vol. 8, pp. 57063–57074, Mar. 2020.

[25] M. Giordani et al., "Toward 6G networks: Use cases and technologies," *IEEE Commun. Mag.*, vol. 58, no. 3, pp. 55–61, Mar. 2020.